J. of Electromagn. Waves and Appl., Vol. 25, 805–818, 2011

TWO-DIMENSIONAL NC-MUSIC DOA ESTIMATION ALGORITHM WITH A CONFORMAL CYLINDRICAL ANTENNA ARRAY

R. Li, L. Xu, X.-W. Shi, L. Chen, and C.-Y. Cui

National Key Laboratory of Science and Technology
on Antennas and Microwaves
Xidian University, P. O. Box 223, Xi'an 710071, China

Abstract—Non-Circular MUSIC (NC-MUSIC) algorithm with a conformal cylindrical array is included to analyze high performance 2-D Direction of Arrival (DOA) estimation. The actual radiation pattern of each microstrip antenna in the conformal array is introduced to analyze the performance of NC-MUSIC algorithm in practice. The simulations show that NC-MUSIC algorithm has a higher resolution than the standard MUSIC algorithm, and the maximum estimation number of NC-MUSIC algorithm is increased, too. In spite of the influence of antennas, NC-MUSIC algorithm achieves 2-D DOA estimation accurately.

1. INTRODUCTION

A number of investigators [1–4] have analyzed a conformal array because it is integrated with the structure and does not cause extra drag. The need for conformal antennas is pronounced for navigation, various communication systems, instrument landing systems, radar altimeter, and large-sized apertures that are necessary for functions as satellite communication and military airborne surveillance radars.

Direction of Arrival (DOA) estimation of signals is important in array signal processing [5–21]. In the literature available, non-circular signals are utilized to enhance the performance of DOA estimation methods [22–27]. Actually, many signals in communication system are non-circular sources, such as the Amplitude Modulation (AM) or Binary Phase Shift Keying (BPSK) signals. For non-circular signals,

Received 10 November 2010, Accepted 30 December 2010, Scheduled 19 January 2011
Corresponding author: Rui Li (ruili@mail.xidian.edu.cn).

the complex symmetric covariance matrix $\mathbf{R}'_{\mathbf{y}} = E(\mathbf{y}_t\mathbf{y}_t^T)$, which is zero for circular signals, where $\mathbf{y}_t$ is the received signal, also contains the second-order statistic characteristics. By exploiting the complex conjugate counterpart of the received signals, the algorithm shows some excellent characters, such as more detectable directions and higher accuracy.

Actually, the directive property of antenna element plays an important role in DOA estimation. Furthermore, each element in the conformal array has a different radiation pattern. Both the directive property and the different radiation pattern caused by conformal array will introduce errors to the array manifold. However, the study of NC-MUSIC method has not been considered with the radiation pattern of the antenna in array, which brings significant errors into the DOA estimation systems.

Although NC-MUSIC algorithm is an excellent algorithm for DOA estimation, there is few paper that implements it to conformal antenna array. In this paper, NC-MUSIC algorithm is applied to a conformal cylindrical array instead of an array of point sources to utilize the directive property of the antenna element. Firstly, a low backlobe microstrip patch antenna is designed, and an 8-element conformal cylindrical array is realized. Secondly, the individual radiation and the mutual coupling among the antennas are introduced into DOA estimation. By this way, we can get a simulation of DOA estimation closer to the practice results. Finally, the character of 2-D DOA estimation with NC-MUSIC algorithm in the conformal antenna system is discussed.

The paper is organized as follows. The conformal cylindrical microstrip patch array is described in Section 2. In Section 3, the performance of NC-MUSIC algorithm with the conformal antenna array is discussed, and numerical simulations are presented in Section 4.

2. A CONFORMAL CYLINDRICAL ARRAY

Antenna array is an important part of a smart antenna system. The conformal cylindrical microstrip antenna array attracts attention more than other shapes, as it features low shape distortions and axial symmetry. A cylindrical array of elements has a potential of 360° coverage, either with an omnidirectional beam, multiple beams, or a narrow beam that can be steered over 360°. A typical application could be a base station antenna in a mobile communication system, resulting in a much more compact installation and less cost.

The conformal cylindrical DOA estimation system is shown in

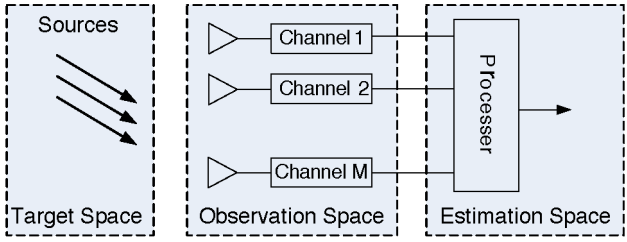

Figure 1. A DOA estimation system.

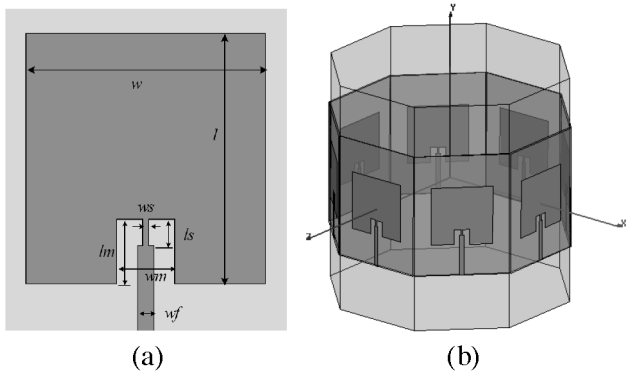

Figure 2. Geometry of the element and array. (a) Geometry of the microstrip patch antenna. (b) Geometry of the conformal cylindrical array.

Fig. 1. It is divided into three parts: spatial signals incident, spatial array receiving and parameter estimation. Correspondingly, it consists of target space, observation space and estimation space. The target space is spanned by non-circular signals and complicated environment parameters. The transform signals from the target space are received by the conformal cylindrical antenna array in the observation space, and the properties of antenna arrays essentially have great effect on DOA estimate. In estimation space, the eigen parameter is extracted from the observation data to compose the target space using NC-MUSIC method.

The basic structure of the cylindrical microstrip patch antenna array is depicted in Fig. 2(a). The array is built up on substrate with $\varepsilon_r = 2.65$ and thickness of 1 mm. The sizes of substrate and ground are 80 mm × 60 mm. A rectangular patch is designed, in order to resonate at the center frequency of 2.4 GHz, yielding its dimensions as $w = 39$ mm, $l = 38.1$ mm, $l_m = 10$ mm, $l_s = 4$ mm, $w_s = 1$ mm,

$w_m = 9.4\,\text{mm}$, $w_f = 2.76\,\text{mm}$. An antenna feed is embedded in the patch, and a stepped impendence transformer is used to realize conjugate matching. Eight patch elements are placed along a circle radius $r = 78\,\text{mm}$ and separated by a uniform angle 45° as shown in Fig. 2(b). The cylinder radius is defined to accommodate the inter-element distance of $d = 2\pi R/8 = 0.5\lambda_0$.

3. NC-MUSIC ALGORITHM WITH A CONFORMAL CYLINDRICAL ARRAY

In this paper, a conformal cylindrical array of M antennas is used as receiver. Let K ($K < M$) narrow band non-circular sources impinge into the array. The non-circular signal can be defined by constellation diagram. If a signal's amplitudes lie on a line in the complex I-Q-diagram, it is called non-circular signal. In addition, the statistical characteristic of non-circular signal is the elliptic covariance matrix $\mathbf{R}'_{\mathbf{x}} E(\mathbf{x}_t \mathbf{x}_t^T) \neq 0$.

The direction of the k-th arriving signal is determined by the azimuth and elevation angles, ϕ_k and θ_k, respectively. The received signal model is modified as following:

$$\mathbf{y}_t = \mathbf{A} \odot \mathbf{E}\mathbf{x}_t + \mathbf{n}_t,\ t = 1, \ldots, T \tag{1}$$

where $\mathbf{A} = [\mathbf{a}_1, \ldots, \mathbf{a}_K]$ is the $M \times K$ steering matrix, and $\mathbf{a}_k = [\mathbf{a}_1(\theta_k, \phi_k), \ldots, \mathbf{a}_M(\theta_k, \phi_k)]^T$, $(k = 1, \ldots, K)$ stands for the phase delay due to propagation of each antenna for the k-th incident signal, which can be deduced from the geometry of antenna array. $\mathbf{E} = [\mathbf{E}_1, \ldots, \mathbf{E}_K]$ is the far zone electric fields of antenna in array, and $\mathbf{E}_k = [E_1(\theta_k, \phi_k), \ldots, E_M(\theta_k, \phi_k)]^T$, $(k = 1, \ldots, K)$ are the far-fields of the array in the direction of (θ_k, ϕ_k). In order to get a more practical DOA estimation result, the pattern of the m-th antenna in conformal array $E_m(\theta_k, \phi_k)$ $(m = 1, \ldots, M)$ is used here which are often ignored in other papers [6–10]. The sign $\odot$ denotes the Schur-Hadamard product. $A \odot B$ is the entry-by-entry product of matrix $\mathbf{A}$ and $\mathbf{B}$. The vector $\mathbf{x}_t = [x_{t,1}, \ldots, x_{t,K}]^T$ models signals transmitted by complex non-circular sources. $\mathbf{n}_t$ denotes spatially white noise. $\mathbf{x}_t$ and $\mathbf{n}_t$ are multivariate independent and zero-mean. And the noise is independent of the incoming signals.

Obviously, the geometry of cylinder, the shape and the location of elements play important roles in the DOA estimation algorithm for conformal antenna array. Based on the analysis of antenna and array, the actual DOA estimation will be carried out with $\mathbf{E}$ and $\mathbf{A}$.

The covariance matrices of $\mathbf{x}_t$ are $\mathbf{R}_{\mathbf{x}} = E(\mathbf{x}_t \mathbf{x}_t^H)$, $\mathbf{R'}_{\mathbf{x}} = E(x_t x_t^T)$. $\mathbf{n}_t$ satisfies $E(\mathbf{n}_t \mathbf{n}_t^H) = \sigma_n^2 \mathbf{I}_M$, $E(\mathbf{n}_t \mathbf{n}_t^T) = 0$. Consequently, this leads

to the covariance matrices of $\mathbf{y}_t$:

$$\mathbf{R}_{\mathbf{y}} \overset{\text{def}}{=} E\left(\mathbf{y}_t\mathbf{y}_t^H\right) = \mathbf{A} \odot \mathbf{E}\mathbf{R}_{\mathbf{x}}\mathbf{E}^H \odot \mathbf{A}^H + \sigma_n^2\mathbf{I}_M \tag{2}$$

$$\mathbf{R}'_{\mathbf{y}} \overset{\text{def}}{=} E\left(\mathbf{y}_t\mathbf{y}_t^T\right) = \mathbf{A} \odot \mathbf{E}\mathbf{R}'_{\mathbf{x}}\mathbf{E}^T \odot \mathbf{A}^T \tag{3}$$

As mentioned above, $\mathbf{R}'_{\mathbf{y}} = \mathbf{0}$ for the case of circular sources and $\mathbf{R}'_{\mathbf{y}} \neq \mathbf{0}$ for the case of non-circular sources. In this paper, the non-circular sources are used to improve the performance of DOA estimation algorithm for conformal array, and the covariance matrices are classically estimated by

$$\mathbf{R}_{\mathbf{y}} = (1/N)\sum_{n=1}^{N}\mathbf{y}_t\mathbf{y}_t^H, \quad \mathbf{R}'_{\mathbf{y}} = (1/N)\sum_{n=1}^{N}\mathbf{y}_t\mathbf{y}_t^T \tag{4}$$

As the unconjugated spatial covariance matrix for non-circular signals contains the second-order statistical characteristics, the covariance matrices $\mathbf{R}_{\mathbf{y}}$ and $\mathbf{R}'_{\mathbf{y}}$ can be utilized to improve the performance of DOA estimation algorithms. To devise subspace-based algorithms built from both $\mathbf{R}_{\mathbf{y}}$ and $\mathbf{R}'_{\mathbf{y}}$, the extended covariance matrix $\tilde{\mathbf{R}}_{\mathbf{y}} = E[\mathbf{Y}\mathbf{Y}^H]$ is considered, where

$$\mathbf{Y} = \begin{bmatrix} \mathbf{y}_t \\ \mathbf{y}_t^* \end{bmatrix} = \begin{bmatrix} \mathbf{A} \odot \mathbf{E} & \mathbf{0} \\ \mathbf{0} & \mathbf{A}^* \odot \mathbf{E}^* \end{bmatrix} \begin{bmatrix} x_t \\ x_t^* \end{bmatrix} + \begin{bmatrix} \mathbf{n}_t \\ \mathbf{n}_t^* \end{bmatrix} \tag{5}$$

$$\tilde{\mathbf{R}}_{\mathbf{y}} = \tilde{\mathbf{A}}\tilde{\mathbf{R}}_{\mathbf{x}}\tilde{\mathbf{A}}^H + \sigma_n^2\mathbf{I}_{2M} \tag{6}$$

With

$$\tilde{\mathbf{A}} \overset{\text{def}}{=} \begin{pmatrix} \mathbf{A} \odot \mathbf{E} & \mathbf{0} \\ \mathbf{0} & \mathbf{A}^* \odot \mathbf{E}^* \end{pmatrix} \text{ and } \tilde{\mathbf{R}}_{\mathbf{x}} \overset{\text{def}}{=} \begin{pmatrix} \mathbf{R}_{\mathbf{x}} & \mathbf{R}'_{\mathbf{x}} \\ \mathbf{R}'^*_{\mathbf{x}} & \mathbf{R}^*_{\mathbf{x}} \end{pmatrix} \tag{7}$$

where * stands for conjugate.

The non-circularity rate ρ_k of the k-th signal is defined by:

$$E\left(\mathbf{x}_{t,k}^2\right) = \rho_k e^{j\varphi_k} E\left|\mathbf{x}_{t,k}\right|^2 = \rho_k e^{j\varphi_k}\varepsilon_k^2, \quad k = 1, 2, \ldots, K \tag{8}$$

And it satisfies $0 \leq \rho_k \leq 1$ (from the Cauchy-Schwartz inequality). The study is concentrated on a particular case $\rho_k = 1$ because very attractive algorithms have been devised for this case [22, 26]. The non-circularity phase $e^{j\varphi_k}$ represents the effect of the channel on the k-th signal (the channel is assumed to be fixed during the estimation period). With Eq. (8), the covariance matrix of uncorrelated non-circular signals can be written as $\mathbf{R}_{\mathbf{x}} = \mathbf{\Pi}_\varepsilon$ and $\mathbf{R}'_{\mathbf{x}} = \mathbf{\Pi}_\varphi\mathbf{\Pi}_\varepsilon$, where $\mathbf{\Pi}_\varepsilon \overset{\text{def}}{=} \text{Diag}(\varepsilon_1^2, \ldots, \varepsilon_K^2)$ and $\mathbf{\Pi}_\varphi \overset{\text{def}}{=} \text{Diag}(e^{i\varphi_1}, \ldots, e^{i\varphi_K})$ [26].

Consequently,

$$\tilde{\mathbf{R}}_{\mathbf{x}} = \begin{pmatrix} \mathbf{\Pi}_\varepsilon & \mathbf{\Pi}_\varphi\mathbf{\Pi}_\varepsilon \\ \mathbf{\Pi}^*_\varphi\mathbf{\Pi}_\varepsilon & \mathbf{\Pi}_\varepsilon \end{pmatrix} = \begin{pmatrix} \mathbf{I}_K \\ \mathbf{\Pi}^*_\varphi \end{pmatrix} \mathbf{\Pi}_\varepsilon \begin{pmatrix} \mathbf{I}_K & \mathbf{\Pi}_\varphi \end{pmatrix} \tag{9}$$

The received signals are given by

$$\begin{aligned}\tilde{\mathbf{R}}_{\mathbf{y}} &= \begin{pmatrix} \mathbf{A}\odot\mathbf{E} \\ \mathbf{A}^*\odot\mathbf{E}^*\Pi_{\varphi}^* \end{pmatrix}\mathbf{R}_{\mathbf{x}}\begin{pmatrix} \mathbf{E}^H\odot\mathbf{A}^H & \Pi_{\varphi} & \mathbf{E}^T\odot\mathbf{A}^T \end{pmatrix}+\sigma_n^2\mathbf{I}_{2M} \\ &= \mathbf{B}\mathbf{R}_{\mathbf{x}}\mathbf{B}^H+\sigma_n^2\mathbf{I}_{2M} \end{aligned} \tag{10}$$

As radiation patterns of the elements in the conformal array are considered, the steering matrix is modified to $\mathbf{B}=\begin{bmatrix} \mathbf{A}\odot\mathbf{E} \\ \mathbf{A}^*\odot\mathbf{E}^*\mathbf{\Pi}_{\varphi}^* \end{bmatrix}$, and $\mathbf{B}=[\mathbf{b}_1,\ldots,\mathbf{b}_K]$, $\mathbf{b}_k=\mathbf{b}_k(\theta_k,\phi_k)$. Because the sizes of the extended steering matrix $\mathbf{B}$ and the extended covariance matrix $\tilde{\mathbf{R}}_{\mathbf{y}}$ are $2M\times K$ and $2M\times 2M$ respectively, the number of antennas is virtually "doubled", which yields in a higher resolution and higher number of separable sources.

NC-MUSIC algorithm is based on the property that the steering vector is orthogonal to the noise subspace. Consequently, the orthogonal projector matrix onto the noise subspace is considered. The eigenvectors matrix $\tilde{\mathbf{U}}_N$ associated with the noise subspace is estimated by using the eigendecomposition of $\tilde{\mathbf{R}}_{\mathbf{y}}=\tilde{\mathbf{U}}\Sigma\tilde{\mathbf{U}}^H$. There are $2M$ diagonal elements in the eigenvalue matrix Σ, and the noise subspace eigenvectors matrix $\tilde{\mathbf{U}}_N$ is composed of eigenvectors associated with the $2M-K$ smallest eigenvalue.

Using NC-MUSIC algorithm based on $\tilde{\mathbf{U}}_N$ and $\mathbf{b}(\theta,\phi)$, the DOAs are estimated as the locations of the K smallest minima of the function

$$\begin{cases} \theta_i=\arg\ \min\limits_{\theta}\mathbf{b}^H(\theta,\phi)\,\tilde{\mathbf{U}}_N\tilde{\mathbf{U}}_N^H\mathbf{b}(\theta,\phi) \\ \phi_i=\arg\ \min\limits_{\phi}\mathbf{b}^H(\theta,\phi)\,\tilde{\mathbf{U}}_N\tilde{\mathbf{U}}_N^H\mathbf{b}(\theta,\phi) \end{cases} \tag{11}$$

So, the spatial spectrum of NC-MUSIC algorithm is

$$P_{MUSIC}=\frac{1}{\mathbf{b}^H(\theta,\phi)\,\tilde{\mathbf{U}}_N\tilde{\mathbf{U}}_N^H\mathbf{b}(\theta,\phi)} \tag{12}$$

The angular position of the m-th element of a conformal cylindrical array is given by $\sigma_m=2\pi\frac{m}{M}, m=1,\ldots,M$. The array manifold vector $\mathbf{a}_k(\theta_k,\phi_k)$ is given by

$$\mathbf{a}_k(\theta_k,\phi_k)=\left[e^{j\frac{2\pi}{\lambda}r\sin\theta_k\cos(\phi_k-\sigma_1)},\ldots,e^{j\frac{2\pi}{\lambda}r\sin\theta_k\cos(\phi_k-\sigma_M)}\right]^T \tag{13}$$

For non-circular sources, adding the field pattern of individual elements the steering vector of a conformal cylindrical antenna array

is extended to

$$\mathbf{b}_k(\theta_k,\phi_k)=\begin{bmatrix} E_1 e^{j\frac{2\pi}{\lambda}r\sin\theta_k\cos(\phi_k-\sigma_1)} \\ \vdots \\ E_M e^{j\frac{2\pi}{\lambda}r\sin\theta_k\cos(\phi_k-\sigma_M)} \\ E_1^* e^{-j\left[\frac{2\pi}{\lambda}r\sin\theta_k\cos(\phi_k-\sigma_1)+\varphi_k\right]} \\ \vdots \\ E_M^* e^{-j\left[\frac{2\pi}{\lambda}r\sin\theta_k\cos(\phi_k-\sigma_M)+\varphi_k\right]} \end{bmatrix} \tag{14}$$

With Eq. (14), Eq. (12) can be carried out to estimate the directions of signals arrival, and the 2-D DOA estimation system is realized with a conformal cylindrical array.

4. SIMULATIONS

In this section, we carry out some representative simulation experiments to demonstrate the validity of NC-MUSIC method for conformal cylindrical array.

Firstly, the character of the microstrip patch antenna and conformal cylindrical array are analyzed. The S_{11} of the antenna is presented in Fig. 3. The center frequency is designed as 2.4 GHz. The gain of the embedded microstrip patch antenna is shown in Fig. 4. Because of the conformal array geometry, the backlobe would decrease the performance of the system. We selected proper sizes to reduce the backlobe as much as possible. It can be seen that the design of the antenna satisfied the requirement. The radiation electric field of all the elements in the array is given in Fig. 5. Using the electric field of antennas in the conformal cylindrical array, the actual DOA estimation can be calculated to get more practical results.

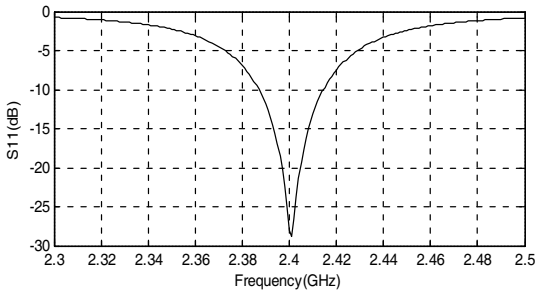

Figure 3. The S_{11} of the 2.4 G microstrip patch antenna.

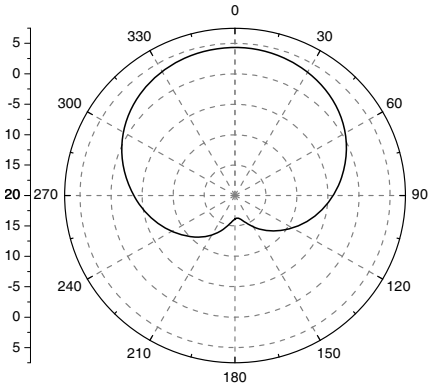

Figure 4. Gain of an embedded microstrip patch antenna.

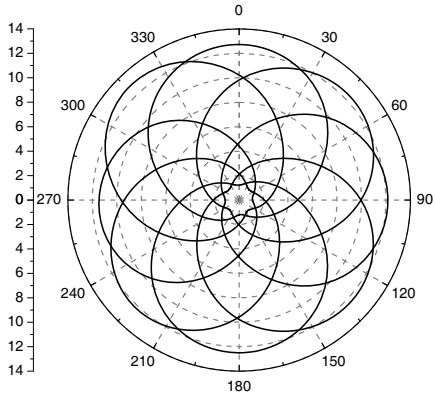

Figure 5. Individual electrical field pattern of 8-element array.

Secondly, in order to verify the performance of NC-MUSIC algorithm, the performances of MUSIC and NC-MUSIC methods are compared in two cases: the Root-Mean-Square-Error (RMSE) VS. signal-to-noise ratio (SNR) and angle separation.

The RMSE of the DOA estimation is defined as

$$\mathrm{RMSE}(k) = \sqrt{\left(\widehat{\theta}_k - \theta_k\right)^2 + \left(\widehat{\phi}_k - \phi_k\right)^2} \tag{15}$$

where $\widehat{\theta}_k$, $\widehat{\phi}_k$ are the estimated values of θ_k, ϕ_k. In all experiments, a BPSK modulation scheme is assumed. Different signal sources are assumed to be mutually uncorrelated. The number of snapshots is 512. 200 independent simulation runs have been performed to obtain the estimation DOAs.

Three sources located at $\theta,\ \phi = [15^\circ, 30^\circ]$, $[20^\circ, 280^\circ]$ and $[70^\circ, 80^\circ]$. Fig. 6 depicts the RMSE of the estimated DOAs as a function of SNR. As expected, the accuracy of DOA estimation improves with increasing SNR. It is also shown that the estimation performance of NC-MUSIC method is superior to the standard MUSIC method, especially in the low SNR.

Then suppose that there were two sources with SNRs of 20 dB impinging on the conformal array from $[\phi_1, \theta_1] = [-(\mathrm{sep}/2)^\circ, -(\mathrm{sep}/2)^\circ]$ and $[\phi_2, \theta_2] = [(\mathrm{sep}/2)^\circ, (\mathrm{sep}/2)^\circ]$. The 'sep' is the separation of the two impinging signals directions. Fig. 7 exhibits the RMSE of the estimated DOAs as a function of the separation of the sources. Generally, the RMSE of NC-MUSIC method is smaller than that of MUSIC method. As angle separation increasing, the RMSE is increased at first

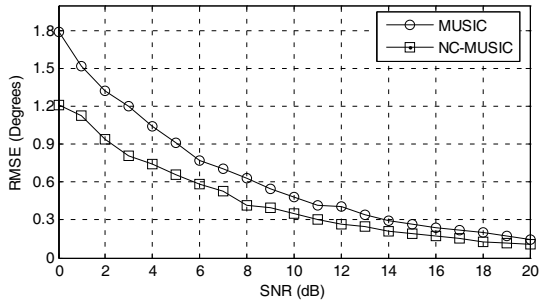

Figure 6. RMSE of the estimated DOAs as a function of SNR.

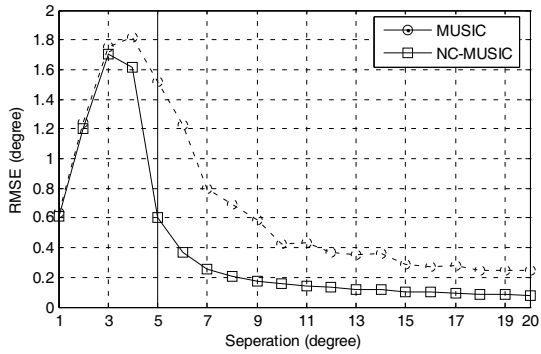

Figure 7. RMSE of the estimated DOAs as a function of the separation.

and then decreased. The explanation is as following. When the sep between two sources is small, it is difficult to detect, and the peak is near the middle of them. It means that the estimated value is close to the real value, so the RMSE is small. When sep increases, the difference between estimated DOA and the real DOA grows which raises the RMSE. When sep is big enough to distinguish the two sources, the RMSE decreases correspondingly. The maximum RMSE of NC-MUSIC method occurs at sep = 3°, and for MUSIC method it occurs at sep = 4°. It is clear that NC-MUSIC method can distinguish sources located more closely.

Thirdly, to examine the influence of a conformal cylindrical array on the performances of NC-MUSIC algorithm, the resolution ability is examined. Four signals with equal power are impinging from the direction at ϕ =[50°, 170°, 210°, 330°]. θ is set to be 90° here. Their SNRs are set at 20 dB. Mutual coupling between the patches has been

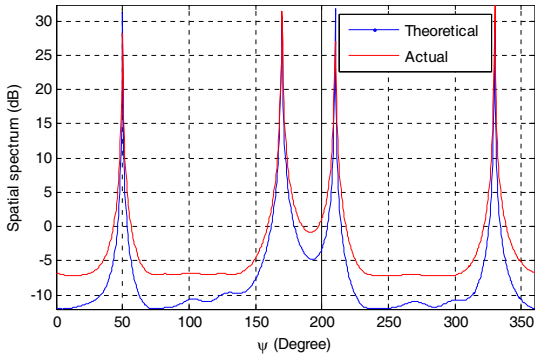

Figure 8. Theoretical and actual DOA estimation of the conformal cylindrical array.

considered in the radiation patterns of antennas in the array. The theoretical spatial spectrum and actual result are compared in Fig. 8. The theoretical result is calculated with point sources. The actual result is obtained with the radiation patterns of antennas in conformal cylindrical array. From the comparison we can see that the spatial spectrum of actual DOA estimation results is not as sharp as that of the theoretical results. The theoretical results are obtained by considering the antenna as point source, which does not match the actual results. That is to say, the radiation pattern of antenna in array has to be included in the design of conformal DOA estimation system.

Fourthly, we discuss the maximum estimation number of NC-MUSIC algorithm with the conformal cylindrical array. Using NC-MUSIC algorithm, an 8-element conformal array is able to estimate 12 sources from the direction separated by a uniform azimuth angle 30° as shown in Fig. 9. The elevation angle is set to be 90° here. In the traditional way, an 8-element array is able to estimate only 7 sources. Actually, NC-MUSIC method doubles the maximum number of estimation sources compared to the number of circular MUSIC method. With the non-circular assumption, the maximum number of detectable sources is up to $2(M-1)$ [22, 23]. The radiation patterns of antennas are considered in this example, which means, the actual conformal antenna array can handle more sources than elements in the array with NC-MUSIC algorithm. This feature can be used to reduce the cost of communication systems.

Finally, benefiting from the conformal cylindrical array, the 2-D DOA estimation with NC-MUSIC methods is realized. Six signals with equal power are impinging from the direction θ, ϕ = [15°, 30°], [20°, 280°], [30°, 120°], [50°, 340°], [60°, 170°] and [70°, 80°]. The

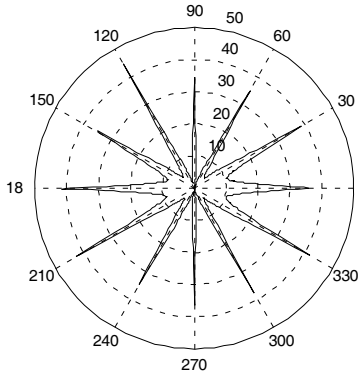

Figure 9. Actual DOA estimation of 12 sources with 8-element array.

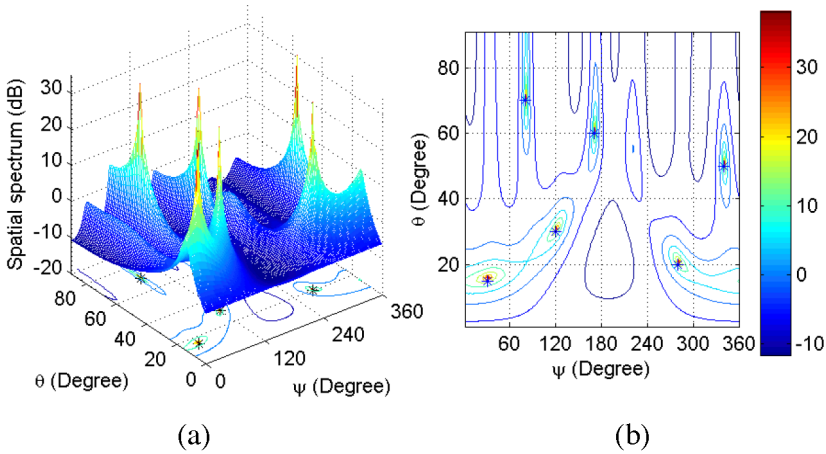

Figure 10. The 2-D spatial spectrum and the contour with the conformal cylindrical array. (a) The 2-D spatial spectrum. (b) The contour of the spatial spectrum.

DOA spatial spectrum is given in Fig. 10(a). To illustrate the estimation results, the contour of spatial spectrum in Fig. 10(a) is shown in Fig. 10(b), and the correct locations of the signals are marked with black stars. The figure shows that the algorithm can estimate azimuth and elevation angles of 6 sources with the conformal cylindrical microstrip antenna array.

5. CONCLUSION

In this paper, a conformal cylindrical microstrip antenna array was designed and investigated. NC-MUSIC algorithm of DOA estimation was applied to this array. The electric fields for each element in the antenna array were analyzed, and the effects of it on NC-MUSIC algorithm were considered. The simulations verified that NC-MUSIC method improved the performance of DOA estimation remarkably and that it could handle more sources than standard methods. Taking into account the radiation pattern of the conformal array, the actual DOA estimation performances were decreased compared to the theoretical results.

ACKNOWLEDGMENT

This work was supported by the National Science Foundation of China under Grant No. 60801039

REFERENCES

1. Josefsson, L. and P. Persson, *Conformal Array Antenna Theory and Design*, Wiley-IEEE Press, 2006.
2. Wincza, K., S. Gruszczynski, and K. Sachse, "Conformal four-beam antenna arrays with reduced sidelobes," *Electronics Letters*, Vol. 44, 174–175, 2008.
3. Chu, L. C. Y., D. Guha, and Y. M. M. Antar, "Conformal strip-fed shaped cylindrical dielectric resonator: Improved design of a wideband wireless antenna," *IEEE Antennas and Wireless Propagation Letters*, Vol. 8, 482–485, 2009.
4. Guo, J. L. and J. Y. Li, "Pattern synthesis of conformal array antenna in the presence of platform using differential evolution algorithm," *IEEE Transactions on Antennas and Propagation*, Vol. 57, 2615–2621, 2009.
5. Lie, J. P., B. P. Ng, and C. M. See, "Multiple UWB emitters DOA estimation employing time hopping spread spectrum," *Progress In Electromagnetics Research*, Vol. 78, 83–101, 2008.
6. Gu, Y. J., Z. G. Shi, K. S. Chen, and Y. Li, "Robust adaptive beamforming for steering vector uncertainties based on equivalent DOAs method," *Progress In Electromagnetics Research*, Vol. 79, 277–290, 2008.
7. Lizzi, L., F. Viani, M. Benedetti, P. Rocca, and A. Massa, "The

M-DSO-esprit method for maximum likelihood DOA estimation," *Progress In Electromagnetics Research*, Vol. 80, 477–497, 2008.

8. Zhang, X., Y. Shi, and D. Xu, "Novel blind joint direction of arrival and polarization estimation for polarization-sensitive uniform circular array," *Progress In Electromagnetics Research*, Vol. 86, 19–37, 2008.
9. Zhang, X., D. Wang, and D. Xu, "Novel blind joint direction of arrival and frequency estimation for uniform linear array," *Progress In Electromagnetics Research*, Vol. 86, 199–215, 2008.
10. Zhang, X., J. Yu, G. Feng, and D. Xu, "Blind direction of arrival estimation of coherent sources using multi-invariance property," *Progress In Electromagnetics Research*, Vol. 88, 181–195, 2008.
11. Tayebi, A., J. Gómez, F. S. Saez de Adana, and O. Gutierrez, "The application of ray-tracing to mobile localization using the direction of arrival and received signal strength in multipath indoor environments," *Progress In Electromagnetics Research*, Vol. 91, 1–15, 2009.
12. Palanisamy, P. and N. Rao, "Direction of arrival estimation based on fourth-order cumulant using propagator method," *Progress In Electromagnetics Research B*, Vol. 18, 83–99, 2009.
13. Tayebi, A., J. Gomez, F. Saez de Adana, and O. Gutierrez, "The application of ray-tracing to mobile localization using the direction of arrival and received signal strength in multipath indoor environments," *Progress In Electromagnetics Research,* Vol. 91, 1–15, 2009.
14. Wu, Y., H. Liu, and H. So, "Fast and accurate direction-of-arrival estimation for a single source," *Progress In Electromagnetics Research C*, Vol. 6, 13–20, 2009.
15. Zhang X., X. Gao, G. Feng, and D. Xu, "Blind joint DOA and DoD estimation and identifiability results for MIMO radar with different transmit/receive array manifolds," *Progress In Electromagnetics Research B*, Vol. 18, 101–119, 2009.
16. Yang, P., F. Yang, and Z. Nie, "DOA estimation with sub-array divided technique and interporlated esprit algorithm on a cylindrical conformal array antenna," *Progress In Electromagnetics Research*, Vol. 103, 201–216, 2010.
17. Zhang, X., G. Feng, and D. Xu, "Blind direction of angle and time delay estimation algorithm for uniform linear array employing multi-invariance music," *Progress In Electromagnetics Research Letters*, Vol. 13, 11–20, 2010.
18. Liao, B., G. S. Liao, and J. Wen, "A method for DOA estimation

in the presence of unknown nonuniform noise," *Journal of Electromagnetic Waves and Applications*, Vol. 22, No. 14–15, 2113–2123, 2008.

19. Poyatos, D., D. Escot, I. Montiel, I. Gonzalez, F. Saez de Adana, and M. F. Catedra, "Evaluation of particle swarm optimization applied to single snapshot direction of arrival estimation," *Journal of Electromagnetic Waves and Applications*, Vol. 22, No. 16, 2251–2258, 2008.
20. Zhang, X., X. Gao, and W. Chen, "Improved blind 2D-direction of arrival estimation with L-shaped array using shift invariance property," *Journal of Electromagnetic Waves and Applications,* Vol. 23, No. 5–6, 593–606, 2009.
21. Park, G., H. Lee, and S. Hong, "DOA resolution enhancement of coherent signals via spatial averaging of virtually expanded arrays," *Journal of Electromagnetic Waves and Applications*, Vol. 24, No. 1, 61–70, 2010.
22. Chargé, P., Y. Wang, and J. Saillard, "A root MUSIC algorithm for non circular Sources," *IEEE ICASSP*, 2985–2988, 2001.
23. Haardt, M. and F. Romer, "Enhancements of unitary ESPRIT for non-circular sources," *IEEE ICASSP*, Vol. 22, 101–104, Montral, QC, Canada, May 2004.
24. Delmas, J. P. and H. Abeida, "Stochastic Cramér-Rao bound for noncircular signals with application to DOA estimation," *IEEE Trans. Signal Processing*, Vol. 52, 3192–3199, Nov. 2004.
25. Delmas, J. P., "Asymptotically minimum variance second-order estimation for noncircular signals with application to DOA estimation," *IEEE Trans. Signal Process.*, Vol. 52, 1235–1241, May 2004.
26. Delmas, J. P. and H. Abeida, "MUSIC-like estimation of direction of arrival for noncircular sources," *IEEE Trans. Signal Processing*, Vol. 54, 2678–2690, Jul. 2006.
27. Gan, L., J.-F. Gu, and P. Wei, "Estimation of 2-D DOA for noncircular sources using simultaneous SVD technique," *IEEE Antennas and Wireless Propagation Letters*, Vol. 7, 385–388, 2008.